Research Square

Preprints are preliminary reports that have not undergone peer review.
They should not be considered conclusive, used to inform clinical practice,
or referenced by the media as validated information.

Mechanisms of River Morphology Influencing Water Self-Purification Capacity: A Physical Model Experimental Study

Chenguang Xiao
Anhui and Huaihe River Institute of Hydraulic Research
Zengyuan Chai
czy@ahwrri.org.cn

Anhui and Huaihe River Institute of Hydraulic Research

Article

Keywords: river morphology, water self-purification capacity, physical model experiments, hyporheic exchange, hydraulic characteristic response factors

Posted Date: June 2nd, 2026

DOI: https://doi.org/10.21203/rs.3.rs-9785776/v1

License: This work is licensed under a Creative Commons Attribution 4.0 International License. Read Full License

Additional Declarations: No competing interests reported.

Abstract

River morphology critically influences water self-purification capacity, yet the pathways of hydraulic response factors remain insufficiently identified. This study employed a multi-form riverbed experimental apparatus to conduct four paired comparisonss: "Mild Slope – Drop Structure," "High Permeability – Low Permeability," "High-Velocity River – Low-Velocity Shallow Lake," and "Obstructed – Unobstructed."Key hydraulic factors and regulatory mechanisms were identified through systematic measurements of total nitrogen (TN) and total phosphorus (TP) removal, flow patterns, velocity distributions, and substrate temperature dynamics. Results show that TN removal was highest in the obstructed and high-velocity river configurations, while TP removal was superior under high-permeability and drop-structure conditions. The low-velocity shallow lake exhibited the poorest removal for both nutrients. River morphology modulates hyporheic exchange intensity by altering flow patterns and velocity fields; substrate temperature variation positively correlates with hyporheic exchange. Seven core hydraulic response factors were identified: flow pattern, velocity, water depth, flow path length, temperature distribution, hyporheic exchange intensity, and biological influence. These factors collectively form an integrated regulatory network. This study reveals a causal chain from river morphology to hydraulic characteristics to self-purification capacity, providing a theoretical basis for river ecological restoration and water environmental capacity enhancement. morphology—hydraulic characteristics—self-purification capacity" and provides a theoretical basis for river ecological restoration and enhancement of water environmental capacity.

0 Introduction

Rivers serve as crucial channels in terrestrial water cycles, acting not only as vital carriers of water resources but also as core ecological systems for pollutant transport and attenuation [1,2]. With accelerated urbanization and intensive industrial and agricultural development, water pollution in rivers has become increasingly prominent. Enhancing river self-purification capacity has thus emerged as a key issue in water environment management and ecological restoration [3,4]. Water self-purification capacity is governed by a multitude of factors, including hydrological processes, hydrodynamic conditions, substrate characteristics, and biological activity [5–7]. Among these, river morphology, as the spatial expression of river channel structure, profoundly influences pollutant mixing, transport, and transformation processes by altering hydraulic characteristics such as flow structure, hydraulic residence time, and hyporheic exchange intensity [8–10].

In recent years, considerable research has been conducted on the impact of river morphology on water quality. Existing studies have shown that geometric features such as sinuosity, slope, and cross-sectional shape significantly affect pollutant transport and mixing processes by modifying velocity distribution and turbulent structure [11–15]. Concurrently, morphological features like substrate permeability and stepped drops have been shown to regulate hyporheic exchange at the water-substrate interface [16,17]. As a key vehicle for mass exchange between overlying water and pore water, hyporheic exchange directly determines the flux of pollutant adsorption and degradation within the substrate[18–20]. However, existing research often focuses on the influence of single morphological factors (e.g., sinuosity, flow velocity) on hydrodynamic or water quality indicators. There is a lack of systematic identification and pathway comparison of various hydraulic response factors under the influence of river morphology. Furthermore, controlled experimental designs based on

physical models are insufficient, hindering the elucidation of the intrinsic mechanisms by which morphological differences affect self-purification capacity.

To address these research gaps, this study employs a self-developed, multi-form movable-bed controlled experimental setup. It establishes several sets of controlled experiments, including "Mild Slope – Drop Structure," "High Permeability – Low Permeability," "High-Velocity River – Low-Velocity Shallow Lake," and "Obstructed – Unobstructed." The study systematically observes response characteristics such as pollutant removal efficiency (TN, TP), flow pattern and velocity distribution, and changes in substrate temperature under different river morphological conditions. It aims to identify the key hydraulic characteristic factors through which river morphology influences water self-purification capacity, and to reveal their pathways and regulatory mechanisms. The findings provide theoretical support and scientific basis for river ecological restoration and the enhancement of water environmental capacity.

1 Methodology

1.1 Experimental System and Setup

This study utilized a multi-form riverbed controlled experimental apparatus. The apparatus consists of two identical experimental tanks to meet the requirements for controlled experiments. Each experimental tank comprises a main channel tank and upstream and downstream water collection tanks. The overall structure is constructed from concrete, with the inner surfaces coated with waterproof paint and lined with waterproof fabric to ensure sealing. The main channel tank has internal dimensions of 350 cm in length, 200 cm in width, and 80 cm in height. The upstream and downstream collection tanks are identical in size, each measuring 60 cm in length, 30 cm in width, and 80 cm in height. An outlet measuring 40 cm × 35 cm is located at the upstream collection tank, leading into the main channel tank, while a 40 cm × 40 cm outlet at the downstream end of the main channel tank discharges into the downstream collection tank. To optimize flow conditions, an energy dissipator is installed at the upstream inlet, and nylon mesh netting is placed at the downstream outlet as a sand trap to prevent sediment from entering the downstream collection tank. A submersible pump with adjustable flow rate is installed inside the downstream collection tank, enabling water circulation via piping. A flow control valve is installed in the pipeline to precisely regulate flow velocity.

1.2 Experimental Design and Procedures

(1) Water Quality Monitoring Experiment: To investigate the self-purification efficiency under different channel morphologies, four sets of controlled experiments were established: "Mild Slope – Drop Structure," "High Permeability – Low Permeability," "High-Velocity River – Low-Velocity Shallow Lake," and "Obstructed – Unobstructed."Each set of experiments was conducted sequentially in the two experimental tanks, with temperature maintained consistently between the control groups using a constant temperature system. The channel simulated the substrate microbial environment of natural river banks. Water bodies with identical, artificially prepared concentrations of TP and TN were used. Each experimental run lasted for 96 hours after initiation, during which water samples were collected at regular intervals for analysis.

(2) Substrate Temperature Change Monitoring: The same batch of river sand was used as the channel substrate across all experiments. To monitor temperature changes within the substrate, multi-probe water temperature data loggers with a sampling frequency reaching the second level were employed. A total of six

temperature measurement points were arranged as follows: Points 1 and 4 were located on the channel centerline; Points 2 and 5 were located on the left bank, 30 cm from the channel boundary; Points 3 and 6 were located on the left bank, 60 cm from the channel boundary. Points 1, 2, and 3 were buried at a depth of 30 cm, while Points 4, 5, and 6 were buried at a depth of 15 cm. The layout for velocity measurement points is shown in Fig. 1. Temperature loggers were buried in the sand substrate at the designated points and connected to a data receiver. Subsequently, water pre-chilled to 5°C was simultaneously injected into the upstream and downstream collection tanks, and the submersible pump flow rate was set to maximum. The data receiver was activated simultaneously with the start of water flow, continuously recording temperature changes at the substrate monitoring points for 6 hours to obtain data from the six points. During the experiment, water temperature was regularly monitored with a thermometer. If the water temperature increased, pre-frozen bottled water was added to the downstream collection tank to maintain the water temperature at approximately 5°C.

(3) Flow Pattern Observation and Flow Velocity Measurement: After completing the temperature experiments, the channel morphology was reconfigured. Under constant flow rate conditions of the submersible pump, foam particles were slowly and uniformly released at the outlet of the upstream collection tank. Their movement trajectories were recorded using a camera to observe the influence of channel morphology on flow patterns. Concurrently, flow velocities were measured at designated points using a velocimeter. Each point was measured three times, and the average value was taken as the final flow velocity.

2 Results and Analysis

2.1 Influence of River Morphology on TN and TP Concentrations

During the 96-hour water quality recirculation monitoring experiment, initial and final concentrations of TN and TP were measured for the four sets of controlled experiments, and removal rates were calculated (Table 1). Additionally, the steady-state reduction intensity at which each control group achieved stable concentrations was calculated (Fig. 2).

For TN, final concentrations showed distinct differentiation depending on channel morphology. The group with flow obstruction achieved the optimal TN removal rate, reaching 82.60%. The drop structure group and the mild slope group exhibited similar TN removal rates, stabilizing between 80.48% and 80.96%, demonstrating relatively balanced removal efficiency. The high-permeability group and low-permeability group achieved TN removal rates of 79.23% and 78.04%, respectively, indicating a slight decrease in TN removal efficiency with reduced substrate permeability. The low-velocity shallow lake group exhibited the lowest TN removal rate at only 66.14%, significantly lower than all other groups.As shown in Fig. 2, the steady-state reduction intensities of TN for Drop Structure, High Permeability, High-Velocity River, and Obstructed are all higher than that of the control group.

For TP, the high-permeability group achieved the highest removal rate at 81.73%, followed closely by the stepped flow group at 81.03%. The low-permeability group and the group with flow obstruction showed moderate removal efficiency, while the mild slope group and low-velocity shallow lake group exhibited the

poorest TP removal performance.As shown in Fig. 2, the steady-state reduction intensities of TP for Drop Structure, High Permeability, High-Velocity River, and Obstructed are all higher than that of the control group.

Table 1
Influence of river morphology on TN and TP concentrations.

control group	TN			TP		
	Initial concentration	Final concentration	Removal rate	Initial concentration	Final concentration	Removal rate
Drop Structure	41.28	7.86	80.96%	1.95	0.37	81.03%
Mild Slope	41.72	8.05	80.70%	2.13	0.46	78.40%
High Permeability	39.76	8.26	79.23%	1.97	0.36	81.73%
Low Permeability	40.25	8.84	78.04%	2.12	0.42	80.19%
High-Velocity River	42.71	14.46	66.14%	1.97	0.78	60.41%
Low-Velocity Shallow Lake	40.52	7.10	82.48%	2.12	0.48	77.36%
Obstructed	40.01	6.96	82.60%	2.32	0.54	76.72%
Unobstructed	40.26	7.86	80.48%	2.16	0.60	72.22%

Overall, the reduction effects of low permeability, mild slope, and low-velocity shallow lake morphologies are relatively weak, particularly that of the low-velocity shallow lake morphology, indicating that drop structures, highly permeable substrates, high-velocity river channels, and obstructive structures are all conducive to water self-purification.

2.2 Influence of Channel Morphology on Water Flow

2.2.1 Influence of Channel Morphology on Flow Pattern

(1) Mild Slope Channel

Using traces left by foam indicator particles in the water, it was observed that after water entered the vertical channel through the inlet, flow velocity was uniform across sections. Flow streamlines were parallel to the channel centerline, with water flowing smoothly through the channel into the downstream collection tank. The flow streamline simulation diagram is shown in Fig. 3.

(2) Channel with Flow Obstruction Structure

Using the traces left by foam indicator particles in the water, it was observed that after the flow entered the channel through the inlet and encountered the obstruction structure, a Kármán vortex street was generated,

with alternating vortices of opposite rotation directions forming downstream of the structure. The flow began to bifurcate and move irregularly towards both sides. Simultaneously, flow velocity increased on both sides of the obstruction structure, resulting in relatively severe erosion of the substrate on both banks. Influenced by the eroded channel sections, the water flowed towards the next obstruction stage before eventually entering the downstream collection tank. The flow streamline simulation diagram is shown in Fig. 3.

(3) Channel with Drop Structure

Using traces left by foam indicator particles, it was observed that after flowing over the drop structure, water fell from a height and flowed towards both sides of the channel, impacting and eroding the substrate on both banks. The water exhibited irregular, multi-directional motion. A depression formed at the inlet; after flowing out of this depression, the water began to flow at a uniform velocity before eventually entering the downstream collection tank. The flow streamline simulation diagram is shown in Fig. 3.

(4) Low-Velocity Shallow Lake Channel

Using traces left by foam indicator particles, it was observed that after entering the channel through the inlet, flow velocity decreased significantly. Water flowed only along the channel margins, with the central section remaining nearly stagnant, before eventually exiting through the outlet into the downstream collection tank. The simulation diagram is shown in Fig. 3.

2.2.2 Influence of Channel Morphology on Flow Velocity

During the flow visualization experiments, a velocimeter was used to measure flow velocities at three locations—inlet, center, and outlet—for the four different channel types, with three measurements taken at each location. The average values were calculated to obtain the flow velocities under the four different channel morphologies, as shown in Table 2.

Table 2
Flow velocities under different channel morphologies

Flow velocity(m/s)	Mild Slope	Obstructed	Drop Structure	Low-Velocity Shallow Lake
Point 1	0.25	0.25	0.17	0.25
Point 2	0.25	0.15	0.28	0.03
Point 3	0.24	0.23	0.25	0.24

Combining flow pattern observations with measurements, the following can be noted:

(1) In the mild slope channel, water flows smoothly from the upstream collection tank to the downstream collection tank. Due to the unidirectional flow direction, uniform velocity distribution across sections, and evenly distributed substrate stress, the impact and erosion of the flow on the substrate are minimal. Consequently, the hyporheic exchange intensity between overlying water and pore water within the substrate is relatively low.

(2) In the channel with flow obstruction structures, these structures increase flow complexity: between the obstructions, flow is impeded and velocity decreases; however, at the edges of the obstructions, the reduction

in cross-sectional area leads to locally accelerated flow. Water flows towards areas of lower velocity, resulting in complex flow directions that impact and erode the substrate, thereby influencing hyporheic exchange between overlying water and pore water.

(3) In the channel with stepped structures, water passing over the steps transitions from smooth flow to vertically downward flow at the inlet, creating a depression and resulting in multi-directional flow. This enhances impact and erosion on the substrate. Concurrently, the conversion of potential energy to kinetic energy accelerates flow velocity, facilitating hyporheic exchange between overlying water and pore water.

(4) In the floodplain channel, due to the sudden increase in cross-sectional area, aside from the uniform flow along the channel margins, the water in the central section is nearly stagnant. This confines most hyporheic exchange between overlying water and pore water to the banks, resulting in relatively weak hyporheic exchange intensity.

Synthesizing the above analysis, it is evident that different channel morphologies influence changes in flow patterns. Changes in flow direction and velocity are critical factors affecting hyporheic exchange intensity between overlying water and pore water. Greater flow complexity and higher flow velocity are associated with stronger hyporheic exchange intensity.

2.3 Influence of River Morphology on Hyporheic Exchange

From the perspective of temperature variation, significant differences in substrate cooling magnitude were observed under different channel morphologies:

Flow Obstruction Structure Group: The group with flow obstruction exhibited the greatest cooling magnitude, with temperature variations at measurement points ranging from 0.3 to 2.0°C. Notably, the temperature decrease at Point 4 reached 2.0°C, the highest value recorded across all experiments. In the group without flow obstruction, temperature variations ranged from 0.2 to 1.6°C, indicating an overall weaker cooling effect compared to the group with obstruction, suggesting that flow obstruction structures facilitate substrate cooling.

Flow Dynamics Group: The drop structure group, mild slope group, and high-velocity channel group demonstrated strong cooling capacity. Temperature variations at core measurement points (Points 4 and 5) were 1.4–1.5°C, 1.5°C, and 1.5°C, respectively, significantly higher than those in the low-velocity shallow lake group (where the variation at Point 4 was only 0.5°C). This indicates that increased flow disturbance intensity and velocity can effectively enhance substrate cooling.

Permeability Group: Both the high-permeability and low-permeability groups exhibited relatively weak overall cooling magnitudes, with temperature variations ranging from 0.1 to 1.2°C and 0.1 to 0.4°C, respectively. The cooling effect was more pronounced in the high-permeability group than in the low-permeability group, suggesting that substrate permeability facilitates cooling.

Low-Velocity Shallow Lake Group: Temperature variations at all measurement points ranged from 0.1 to 0.5°C, representing the smallest cooling magnitude among all experimental groups. This reflects characteristics of higher substrate temperature stability and weaker thermal exchange under slow, quiescent flow conditions.

Additionally, all experimental groups exhibited consistent spatial differences: the temperature decreases at Points 4 and 5 were significantly greater than at other points, identifying these as sensitive zones for substrate thermal exchange. Temperature variations at Points 1–3 and Point 6 were relatively smaller, reflecting spatial heterogeneity in substrate temperature distribution. This indicates that within the three-dimensional space centered on the channel, hyporheic exchange intensity is negatively correlated with distance from the riparian substrate: the closer the substrate is to the channel, the stronger the hyporheic exchange intensity between overlying water and pore water, and vice versa.

Table 3
Comparison Table of Substrate Temperature Variation Rates Under Different Channel Morphologies.

Control group	Point 1	Point 2	Point 3	Point 4	Point 5	Point 6	Mean	Temperature Change Difference
Drop Structure	1.81%	1.08%	1.07%	5.04%	5.38%	1.43%	2.63%	0.66%
Mild Slope	1.85%	0.74%	0.37%	5.56%	2.21%	1.11%	1.97%	
High Permeability	1.55%	0.77%	0.38%	4.65%	2.71%	1.53%	1.93%	1.07%
Low Permeability	0.78%	0.39%	0.40%	1.60%	1.20%	0.79%	0.86%	
High-Velocity River	1.51%	0.75%	0.38%	5.66%	1.50%	1.13%	1.82%	1.01%
Low-Velocity Shallow Lake	0.76%	0.38%	0.38%	1.89%	0.75%	0.75%	0.82%	
Obstructed	3.53%	1.94%	1.15%	7.75%	4.67%	2.34%	3.56%	0.94%
Unobstructed	2.76%	1.17%	0.78%	6.27%	3.16%	1.57%	2.62%	

As shown in Table 3, the average temperature change rates of drop structure, high permeability, high-velocity river, and obstructed were all higher than those of their corresponding control groups, with notably greater variation observed at multiple measurement points, reflecting stronger hyporheic exchange intensity.

The average value for drop structure was 2.63%, exceeding that of mild slope (1.97%), with particularly pronounced increases at measurement points 4 (5.04%) and 5 (5.38%), indicating that aeration and hydraulic disturbance induced by the drop structure enhanced substrate temperature response and promoted hyporheic exchange. The average value for high permeability (1.93%) was significantly higher than that of low permeability, confirming the positive effect of enhanced permeability on hyporheic exchange. The average value for high-velocity river was 1.82%, higher than that of low-velocity shallow lake (0.82%), reaching 5.66% at measurement point 4, demonstrating the enhancing effect of high flow velocity on localized hyporheic exchange. Obstructed exhibited an average temperature change rate of 3.56%, significantly higher than that of unobstructed (2.62%), with particularly notable variations at measurement points 4 (7.75%) and 1 (3.53%), indicating that obstructive conditions effectively enhanced heat exchange between the flow and the substrate, indirectly reflecting stronger hyporheic exchange capacity.

Greater temperature variation within a control group indicates stronger hyporheic exchange intensity, and stronger hyporheic exchange intensity implies greater water self-purification capacity. This further confirms that hyporheic exchange intensity is a key factor influencing water self-purification capacity; its modulation by channel morphology directly determines the efficiency of pollutant migration and transformation at the substrate-water interface [21].

2.4 Identification and Influence Analysis of River Hydraulic Characteristic Response Factors

Through laboratory physical model experiments, including "mild slope – drop structure," "high permeability – low permeability," "high-velocity river – low-velocity shallow lake," and "obstructed – unobstructed." combined with observations of natural river morphologies in the field and findings from prior research [22,23]], the hydraulic characteristic response factors of river morphology and their influences were identified and summarized.

It was identified that river morphology primarily influences the ecological functions and self-purification capacity of water bodies by regulating the following seven core hydraulic characteristic response factors:

 Flow Pattern: Determines the mode of flow energy dissipation and the efficiency of pollutant mixing.

 Flow Velocity: Affects pollutant transport capacity and sediment resuspension.

 Water Depth: Interacts with flow velocity to influence light penetration, aquatic plant growth, and habitat type.

 Flow Path Length: Determines hydraulic residence time, affecting the extent of biochemical reactions.

 Water Temperature Distribution: Acts as a key environmental factor, regulating microbial activity and chemical reaction rates.

 Hyporheic Exchange Intensity: Represents a crucial physical process connecting overlying water and pore water, directly controlling the flux of pollutants into the substrate for adsorption and degradation.

 Biological Influence: Shapes biological habitats, determining the distribution and functions of purifying agents such as microorganisms and plants.

Table 4
River hydraulic characteristic response factors and their influences.

Hydraulic Characteristic Response Factor	Influence
Flow pattern characteristics	Determine the mode of flow energy dissipation and the efficiency of pollutant mixing
Flow velocity characteristics	Affect pollutant transport capacity and sediment resuspension
Water depth characteristics	Influence light penetration, aquatic plant growth, and habitat type
Flow path length	Determines hydraulic residence time and affects the extent of biochemical reactions
Water temperature	Regulates microbial activity and chemical reaction rates
Hyporheic exchange	Key physical process connecting overlying water and pore water; controls the flux of pollutants into the substrate for degradation
Biological influence	Shapes biological habitat environments; determines the distribution and functions of purifying agents such as microorganisms and plants

3 Discussion

Integrating the monitoring and observational results from natural river channel morphologies with findings from prior research, the mechanisms by which river morphology influences water self-purification capacity are analyzed.

River morphology is a core natural factor regulating water self-purification capacity, acting through the modification of a suite of hydraulic characteristic response factors. Specifically, straight channels are characterized by steady, nearly uniform flow, with high and uniformly distributed flow velocity, relatively shallow and uniform water depth along the channel, short flow path length, uniformly mixed water temperature with small vertical temperature differences, weak and localized hyporheic exchange, and low biodiversity due to homogeneous habitats. These characteristics result in strong pollutant transport capacity but insufficient self-purification reactions. The mechanism by which river morphology influences water self-purification capacity is illustrated in Fig. 3.

Meandering channels exhibit flow patterns with alternating impacts on the left and right banks. Flow velocity is generally reduced, characterized by slow flow at convex banks and faster flow at concave banks. Water depth shows a pattern of shallowness at convex banks and depth at concave banks, with an overall increase. Flow path length is significantly increased. Thermal stratification may occur. Longitudinal hyporheic exchange intensity is increased at convex banks, and alternating aerobic and anaerobic environments for microorganisms are provided, greatly promoting pollutant degradation and transformation [23–25].

Drop structure morphology generates free jets and intense turbulence, with localized sharp increases in flow velocity [9]. Water depth decreases in the nappe zone and increases in the impact zone. Flow path length increases slightly. Water temperature decreases and becomes more uniform. This morphology significantly

enhances vertical hyporheic exchange and provides high-oxygen, rapid-flow habitats, strengthening pollutant mixing and aerobic degradation processes [26,27].

Shallow lake morphology is characterized by diffusive flow and weak circulation. Flow velocity is significantly reduced, water depth is generally shallow, flow path length is increased, and thermal gradient circulation can easily form. Hyporheic exchange involves a large area but with weak unit intensity. This morphology provides extensive shallow water and stagnant water habitats, primarily promoting purification by prolonging hydraulic residence time [28,29].

Permeable channels feature coupled surface flow and seepage flow patterns. Surface flow velocity is reduced, water depth decreases slightly, and flow path length remains unchanged. Thermal exchange with pore water is enhanced, and both vertical and lateral hyporheic exchange are significantly enhanced, greatly improving water-substrate-biota connectivity [9]. This provides superior conditions for pollutant entry into the substrate for degradation.

Flow obstruction structures induce flow separation around the obstruction and wake vortex streets. Flow velocity increases locally, water level rises upstream of the structure with local increases in depth, and flow path length increases slightly. Temperature differences may occur upstream and downstream of the structure. Hyporheic exchange is enhanced around the structure, providing attachment substrates for biota and creating retention habitats. Local purification is promoted through physical retention and biological action.

In summary, various river morphologies, by shaping unique combinations of flow pattern, velocity, water depth, flow path length, temperature structure, hyporheic exchange intensity and mode, and biological habitat environment, comprehensively determine pollutant transport capacity, mixing efficiency, hydraulic residence time, microbial activity, and biochemical reaction pathways. Together, these constitute the complex and efficient self-purification mechanisms of river water bodies.

4 Conclusions

This study systematically investigated the mechanisms by which river morphology influences water self-purification capacity using a self-developed, multi-form movable-bed controlled experimental apparatus. The main conclusions are as follows:

(1) River morphology significantly affects pollutant removal efficiency. Flow obstruction structures exhibited the optimal removal effect for TN. High-permeability substrates and the drop structure achieved better removal of TP. The low-velocity shallow lake group demonstrated significantly lower removal capacity for both nitrogen and phosphorus pollutants compared to other morphologies, representing the poorest purification performance.

(2) River morphology significantly regulates hyporheic exchange intensity by altering flow patterns and velocity distributions. Vertical channels, characterized by steady flow and uniform velocity, exhibited relatively low hyporheic exchange intensity. Flow obstruction and stepped structures increased flow complexity and local velocity, enhancing substrate impact and erosion, which facilitated mass exchange between overlying water and pore water. In low-velocity shallow lake group, due to the sudden increase in cross-sectional area and nearly stagnant flow in the central region, hyporheic exchange was concentrated near the banks, resulting in

overall weak exchange intensity. Substrate temperature variation was positively correlated with hyporheic exchange intensity, with greater cooling magnitude indicating stronger hyporheic exchange.

(3) Seven core hydraulic characteristic response factors through which river morphology regulates water self-purification capacity were identified: flow pattern, flow velocity, water depth, flow path length, water temperature distribution, hyporheic exchange intensity, and biological influence. These factors collectively determine pollutant transport capacity, mixing efficiency, hydraulic residence time, microbial activity, and biochemical reaction pathways, forming an integrated regulatory network for river water self-purification capacity.

(4) The mechanism of river morphology's influence was elucidated. As a primary regulatory factor, river morphology shapes distinct hydraulic characteristics, ultimately affecting water self-purification capacity. Straight channels exhibit strong pollutant transport capacity but insufficient self-purification reactions. Meandering channels enhance degradation efficiency by increasing flow path length and longitudinal hyporheic exchange. Stepped structures strengthen turbulence and aerobic degradation. Shallow lake morphology prolongs hydraulic residence time. Permeable channels enhance water-substrate interactions. Flow obstruction structures promote purification through local retention and biological attachment.

In conclusion, river morphology is a key natural factor regulating water self-purification capacity. Through the synergistic action of multi-dimensional hydraulic characteristic response factors, it systematically influences pollutant mixing, transport, transformation, and degradation processes. The findings of this study provide a theoretical basis and scientific support for river ecological restoration, water environmental capacity assessment, and the optimization of channel morphology design.

Declarations

Conflicts of Interest:

The authors declare no conflict of interest.

Funding:

This research was funded by National Natural Science Foundation of China (grant number 52209002); and Natural Science Foundation of Anhui Province (grant number 2208085US09).

Author Contribution

Conceptualization, C.X.and Z.C.; methodology, C.X.and Z.C.; investigation, C.X.and Z.C.; resources, C.X.; data curation, Z.C.; writing—original draft preparation, Z.C.; writing—review and editing, C.X. and Z.C.; project administration, C.X.and Z.C.; funding acquisition, C.X. All authors have read and agreed to the published version of the manuscript.

Data Availability

All data supporting the findings of this study are available in the paper and its supplementary information

References

1. Xu, Z. et al. Theoretical basis and calculation method for ecological base flow for rivers: case study in the Guanzhong reach of the Wei River. *Science Beijing China (in Chinese)* (2016).
2. Nienhuis, J. et al. vol 577, pg 514,. Global-scale human impact on delta morphology has led to net land area gain *Nature (London)*, (2020). https://doi.org/10.1038/S41586-022-05079-0. (2022).
3. Arfa, A., Ayyoubzadeh, S. A., Moghadam, H. S. & Mianabadi, H. Transboundary hydropolitical conflicts and their impact on river morphology and environmental degradation in the Hirmand Basin, West Asia. *Sci. Rep.* **15**, 2754–2754. 10.1038/s41598-024-84501-1 (2025).
4. Martin, G., Christoph, H. & Gregory, E. The third dimension in river restoration: how anthropogenic disturbance changes boundary conditions for ecological mitigation. *Sci. Rep.* **10**, 13106. 10.1038/s41598-020-69796-0 (2020).
5. Domenica, M., Donatella, C., Teresa, C. M. & Marco, O. Assessing the fluvial system resilience of the river Bacchiglione to point sources of pollution in Northeast Italy: a novel Water Resilience Index (WRI) approach. *Environ. Sci. Pollut. Res. Int.* **28**, 36775–36792. 10.1007/s11356-021-13157-5 (2021).
6. S., V. Healthy rivers need diversity, too. *Science* **347**, 516–516, (2015). 10.1126/science.347.6221.516-a
7. Xie, J., Graham, N., Yu, W., Sun, K. & Liu, T. Characterizing natural separation and purification during rural polluted water self-purification in the Dashi River: a multidimensional approach to DOM and microbial interactions. *Separation Purif. Technology*, **136553** (2025).
8. E., P. L. Morphodynamics of Boulder-Bed Semi-Alluvial Streams in Northern Fennoscandia: A Flume Experiment to Determine Sediment Self-Organization. *Water Resour. Research* **57**, (2021). 10.1029/2020wr028859
9. Xiao, C., Chai, Z., Tang, S. & Song, X. Impact of river morphology on water self-purification capacity. *Water Reuse*. 10.2166/wrd.2026.135 (2026).
10. Nick d. G. Human activities have changed the shapes of river deltas. *Nature* **577**, 473–474. https://doi.org/10.1038/d41586-020-00047-y (2020).
11. Monjardin, C. E. F., Power, C. & Senoro, D. B. Spatio-Temporal Assessment of Manganese Contamination in Relation to River Morphology: A Study of the Boac and Mogpog Rivers in Marinduque, Philippines. *Sustainability* 15, (2023). https://doi.org/10.3390/SU15108276
12. Woodward, G. et al. Continental-Scale Effects of Nutrient Pollution on Stream Ecosystem Functioning. *Science* **336**, 1438–1440. https://doi.org/10.1126/science.1219534 (2012).
13. Wei, G. et al. Impact of dam construction on water quality and water self-purification capacity of the Lancang River, China. *Water Resour. Manage*. **23**, 1763–1780 (2009).
14. Liu, X. et al. Flow Dynamics and Contaminant Transport in Y-Shaped River Channel Confluences. *Int. J. Environ. Res. Public Health*. **16**, 572–572. 10.3390/ijerph16040572 (2019).

15. Ishlinsky Institute for. Problems in Mechanics, R. A. o. S. & Water Problems Institute, R. A. o. S. River Flow Structure and Its Effect on Pollutant Distribution. *Water Resources* 46, 910–918, (2019). 10.1134/s0097807819060022
16. Zizeng, L., Hai, Y. & Huiming, C. Influence of fillers on the removal of rainwater runoff pollutants by a permeable brick system with a frame structure base. *Water Sci. technology: J. Int. Association Water Pollution Res.* **80**, 2131–2140. 10.2166/wst.2020.021 (2019).
17. Su, J. et al. Hydro-environmental and ecological effects of drop structure in urban river system. *Water Res. X*. **30**, 100515–100515. 10.1016/j.Wroa.2026.100515 (2026).
18. Sadiq, A. & Singh, K. Slope curvature and pool-riffle interactions drive hierarchical hyporheic exchange: A predictive framework for river corridor management. *Adv. Water Resour.* **209**, 105232–105232. 10.1016/j.Advwatres.2026.105232 (2026).
19. Zhang, Y. et al. Effect of sediment particle size distribution characteristics on hyporheic exchange under different riverbed topography. *J. Hydrol.* **653**, 132752–132752. 10.1016/j.Jhydrol.2025.132752 (2025).
20. Dou, C., Xia, J., Zu, J., Wang, Y. & Yang, M. Effect of point bar on hyporheic exchange within riparian zone: Laboratory experiments. *J. Hydrol.* **643**, 132046–132046. 10.1016/j.Jhydrol.2024.132046 (2024).
21. Yuzhu, L., Chengpeng, L., Chengcheng, W., Bo, L. & Longcang, S. Hyporheic exchange and nitrogen cycle processes under the dual effects of flooding and heterogeneous streambed. *J. Hydrol.* **626** 10.1016/j.Jhydrol.2023.130188 (2023).
22. Xiao, C., Chen, J., Chen, D. & Chen, R. Effects of river sinuosity on the self-purification capacity of the Shiwuli River, China. *Water Supply*. **19**, 1152–1159. https://doi.org/10.2166/ws.2018.166 (2019).
23. Xiao, C. et al. Research on the Influence of River Morphological Changes on Water Self-Purification Capacity: A Case Study of the Shiwuli River in Chaohu Basin. *Water* **17**, 1694. https://doi.org/10.3390/w17111694 (2025).
24. Chenguang, X., Jing, C., Dan, C., Ruidong, C. & Xia, S. Mechanism of sinuosity effect on self-purification capacity of rivers. *Environ. Sci. Pollut. Res. Int.* **30**, 112184–112193. 10.1007/s11356-023-30285-2 (2023).
25. Xiao, C., Chen, J., Yuan, X., Chen, R. & Song, X. Model Test of the Effect of River Sinuosity on Nitrogen Purification Efficiency. *Water* 12, (2020). https://doi.org/10.3390/w12061677
26. He, J., Hou, Q., Lian, J., Jia, W. & Ren, P. High-speed aerated jet trajectory simulated by compounding method of Euler-Euler model and meshless SPH method. *Eng. Appl. Comput. Fluid Mech.* **19** 10.1080/19942060.2025.2545891 (2025).
27. Dong, Y. et al. A Study on the Shape of Parabolic Aeration Facilities with Local Steepness in Slow Slope Chutes. *Water* **16**, 1574. 10.3390/w16111574 (2024).
28. Liu, W. C., Liu, H. M. & Chiu, C. Y. Investigating suspended-sediment transport in a shallow lake using a three-dimensional hydrodynamic and sediment model. *J. Earth Syst. Sci.* **128**, 29. 10.1007/s12040-018-1063-8 (2019).
29. Feng, C. et al. Microbial community dynamics in shallow-water grass-type lakes: Habitat succession of microbial ecological assembly and coexistence mechanisms. *Ecotoxicol. Environ. Saf.* **291**, 117819. 10.1016/j.Ecoenv.2025.117819 (2025).

Figures

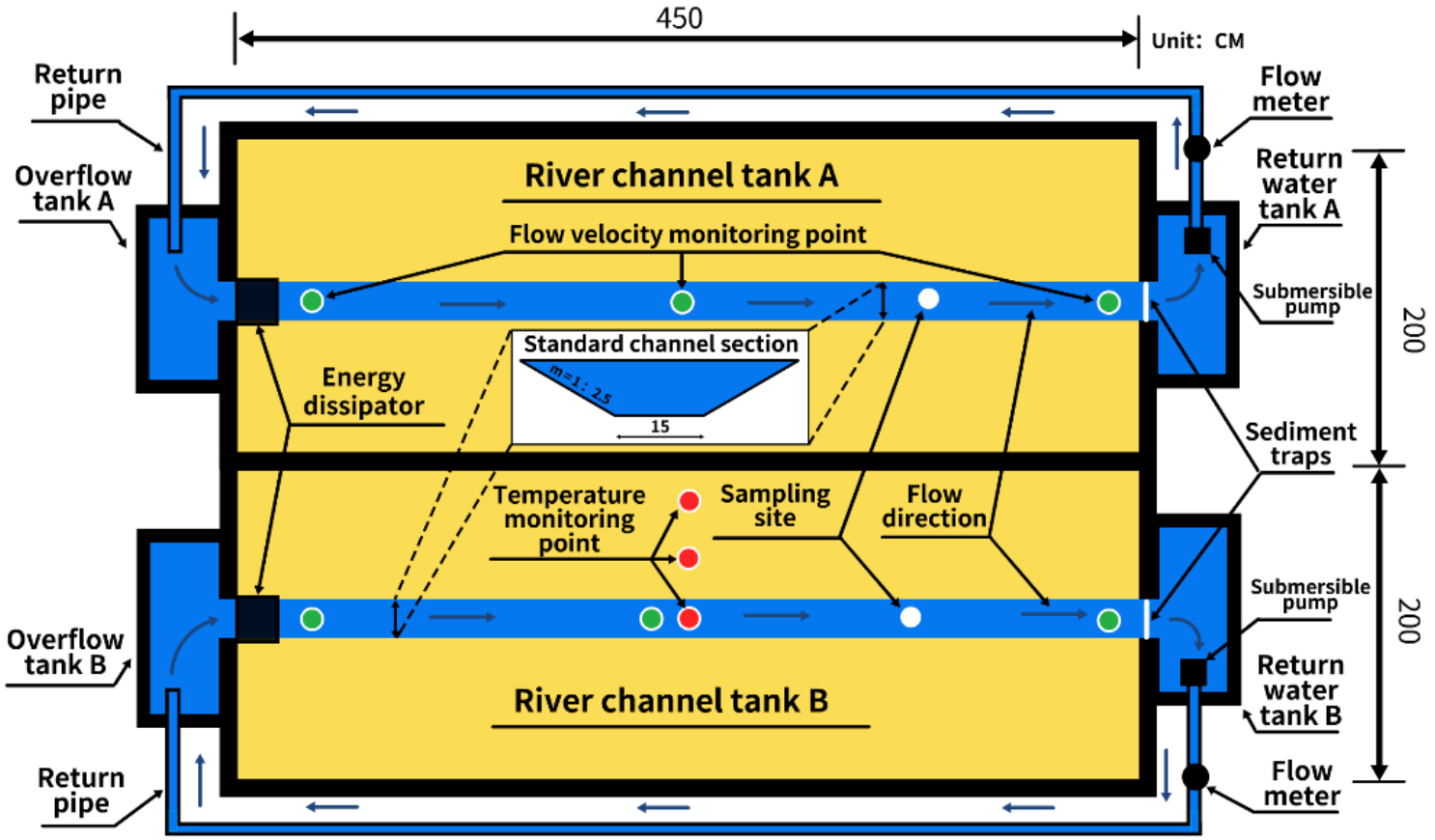


Figure 1

Multi-form riverbed controlled experimental apparatus.

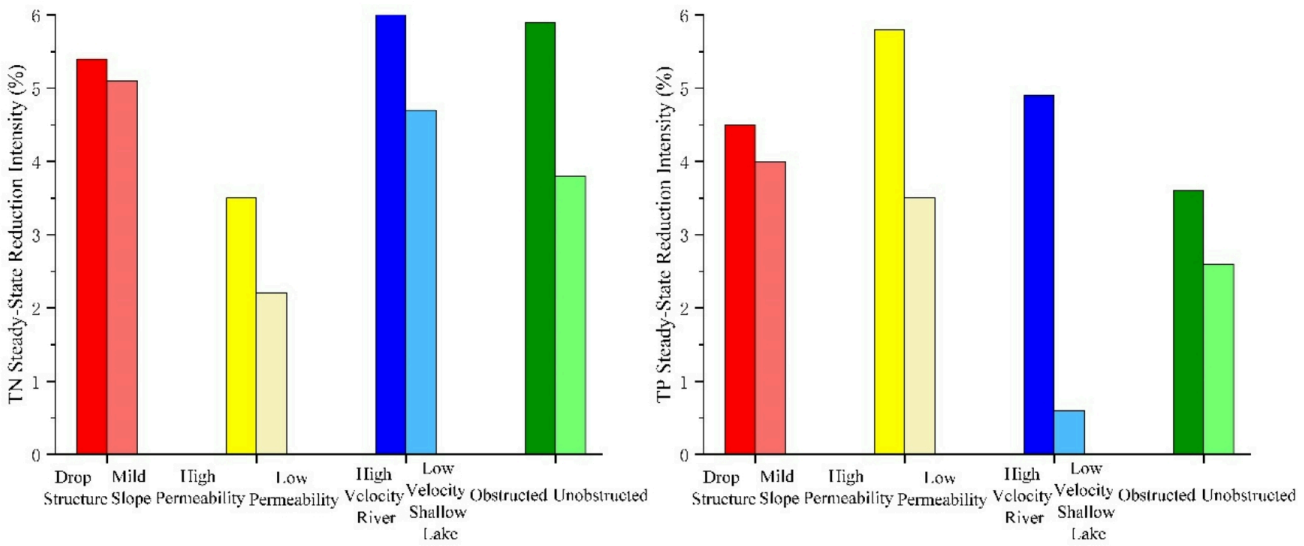


Figure 2

Steady-state reduction intensity of TN and TP under different river morphologies.

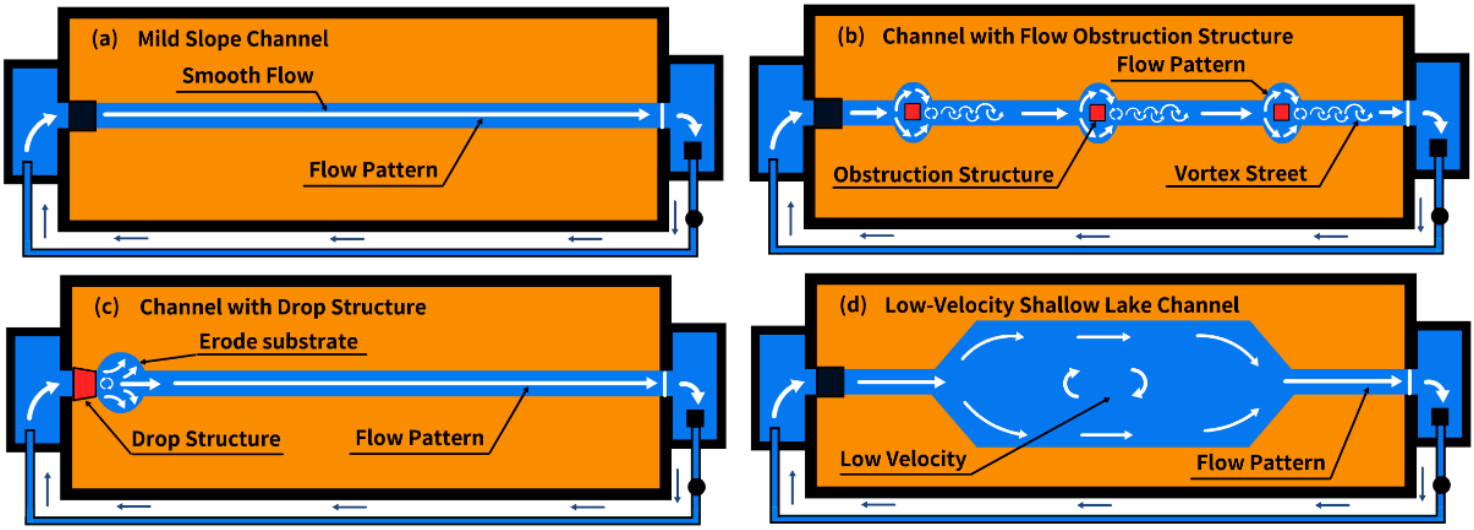


Figure 3

Simulated flow streamlines of the channel.(a) Mild Slope Channel, (b) Channel with Flow Obstruction Structure, (c) Channel with Drop Structure, (d) Low-Velocity Shallow Lake Channel.

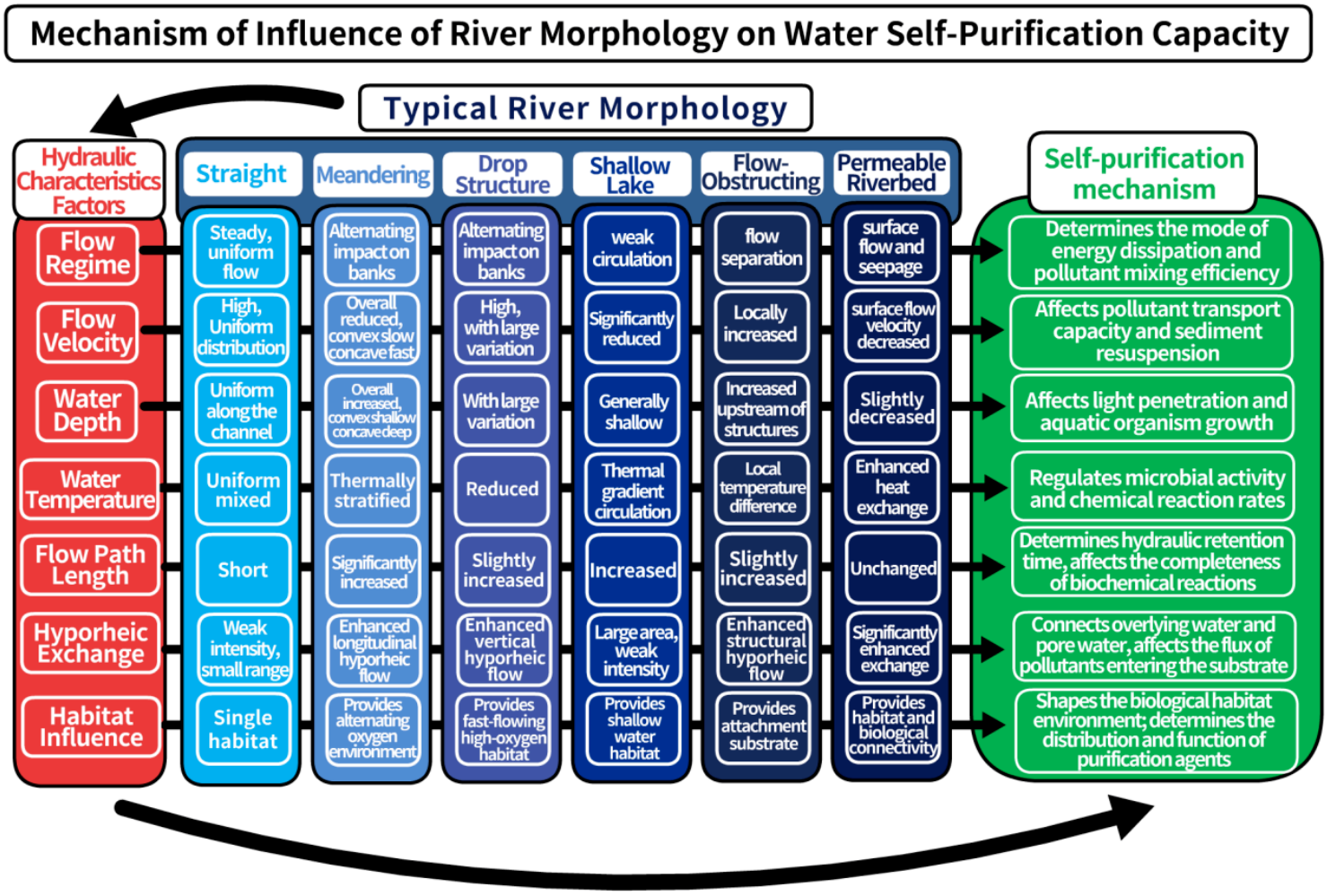


Figure 4

Mechanism of river morphology influence on water self-purification capacity.